Chloryl Nitrate: A Novel Product of the OClO + NO_3 + M Recombination

Randall R. Friedl,* Stanley P. Sander,

Jet Propulsion Laboratory, California Institute of Technology, Pasadena, California 91109

and Yuk L. Yung

Division of Geological and Planetary Sciences, California Institute of Technology, Pasadena, California 91125
(Received: May 20, 1992; In Final Form: July 16, 1992)

The products of the reaction of OClO with NO_3 were investigated between 220 and 298 K using a flow reactor and infrared, visible, and ultraviolet analysis. At temperatures below 250 K new infrared and ultraviolet absorption features were observed and assigned to the novel compound chloryl nitrate (O_2ClONO_2). Additionally, ClO and NO_2 were observed as reaction products, indicating the existence of a second reaction channel. O_2ClONO_2 formation predominates at temperatures below 230 K. The reaction rate constant at 220 K is estimated to be on the order of 10^{-14} cm^3 $molecule^{-1}$ s^{-1} in 1-5 Torr of helium. These observations suggest that O_2ClONO_2 may exist in the terrestrial stratosphere.

Introduction

The discovery of dramatically elevated concentrations of ClO and OClO in the polar stratosphere has focused increased attention on the chemistry of the oxides of chlorine.[1-3] Formation of higher oxides has been actively considered; one higher oxide, Cl_2O_2, is believed to play a critical role in chlorine-catalyzed destruction of polar ozone.[4] Other oxides, such as Cl_2O_3, Cl_2O_4, Cl_2O_6, and Cl_2O_7, have been postulated to serve as temporary reservoirs of chlorine during the early springtime.[5]

An understanding of the partitioning of atmospheric chlorine between reactive and inactive forms is essential for quantitative modeling of polar ozone depletion. Initiation of perturbed chlorine chemistry in the polar atmosphere is thought to occur when inactive chlorine reservoir species HCl and $ClONO_2$ are converted to photochemically labile Cl_2 and HOCl by heterogeneous reactions occurring on polar stratospheric clouds. Many mechanistic issues regarding the actual chemistry on polar stratospheric clouds remain unresolved, however. Atmospheric modeling has been further hindered by the lack of observational data on chlorine reservoir species in the stratosphere. In particular, the temporal and spatial behaviors of the atmospheric abundances of HCl and $ClONO_2$ are poorly characterized by field measurements. The existence of other important chlorine reservoir species cannot, at this time, be excluded by the present observational data base.

We have observed new infrared and ultraviolet spectral features arising from the reaction

$$OClO + NO_3 \rightarrow \text{products} \qquad (1)$$

below temperatures of 250 K. We assign these features to chloryl nitrate (O_2ClONO_2), a compound of potential atmospheric significance whose existence was suggested earlier by Christe et al.[6] In this report we present a characterization of the products of reaction 1 and evidence in support of the assignment of chloryl nitrate.

Experimental Section

Detection of reactants and products was accomplished by long-path absorption in a 1.5-m-long (15-cm-diameter), temperature-controlled, gaseous flow reactor. NO_3 was generated in an upstream prereactor by the reaction of F atoms with HNO_3 or Cl atoms with $ClNO_3$. Atomic species were produced by microwave discharge of diatomic precursors. The procedure for synthesizing and handling HNO_3 and $ClNO_3$ has been discussed previously.[7] OClO was prepared by passage of Cl_2 through slightly moist $NaClO_2$ and trapped at 195 K. Products more volatile than OClO such as Cl_2 were pumped off. A slow flow of helium carried OClO (approximately 1 Torr vapor pressure at 195 K) into the flow system through a small tubular injector. Using this procedure, products that are less volatile than OClO, including water, remain in the trap. No detectable impurities in the OClO sample were observed using infrared and ultraviolet absorption.

Some additional experiments were performed on the reactions of NO_3 with Cl and ClO. In these experiments ClO was produced by reaction of Cl with Cl_2O. The Cl_2O was produced by passage of Cl_2 through HgO.

We conducted experiments between 220 and 298 K and 1 and 8 Torr total pressure of helium buffer gas. The gaseous residence time within the reactor ranged between 1 and 4 s. Total flow rates were between 2 and 6 SLM. Spectroscopic interrogation of the reactor contents was accomplished using a previously described optical arrangement.[8] The infrared optical system consisted of a Bomem DA3+.002 Fourier transform infrared spectrometer coupled to White-type optics in the flow tube (1.5-m base path, 42-m optical path length) and a liquid helium-cooled Cu:Ge detector. The UV/visible optical system consisted of a D_2 or quartz-halogen lamp coupled through the flow tube (1.5-m optical path length) to a diode array spectrometer (PARC 1461/1412 OMA III; 600 grooves/mm grating monochromator) with a 150-nm bandwidth.

The optical systems integrate gaseous absorption along the flow tube axis. The temperature-controlled reactor section encompasses approximately 90% of the optical path. To ensure a uniform reaction temperature, NO_3 was injected at the rear of the reaction cell while OClO was injected approximately 10 cm downstream, at the beginning of the temperature-controlled region. Intregrated absorbances obtained for initial concentrations of NO_3 ranged between 0.02 and 0.3 (as measured at the 662-nm band peak); for OClO they were between 0.05 and 0.4 (at the 351.3-nm band peak). These absorbances correspond to average flow tube concentrations of $(0.6-10) \times 10^{13}$ cm^{-3} for NO_3 and $(2-17) \times 10^{13}$ cm^{-3} for OClO.

Results and Discussion

The coaddition of NO_3 and OClO in the reactor resulted in nearly complete disappearance (>90%) of the visible NO_3 absorption spectrum regardless of the experimental temperature or the ratio of NO_3 and OClO initial concentrations (varied between 5:1 and 1:5). In contrast, the ultraviolet OClO absorbance decreased slowly with increasing NO_3 concentration, reaching a minimum value of one-third the initial value (at the highest NO_3:OClO ratio). These observations suggest the occurrence of a multiple path or catalytic chain mechanism that effectively destroys NO_3 but conserves OClO. The kinetics of this process are constrained by the absorbance data obtained for NO_3. On the basis of the optical data, we estimate that the first-order removal rate of NO_3 was between 1 and 5 s^{-1} for the range of OClO concentrations. The corresponding bimolecular rate coefficient for reaction 1, assuming it to be the rate-limiting step,

0022-3654/92/2096-7490$03.00/0

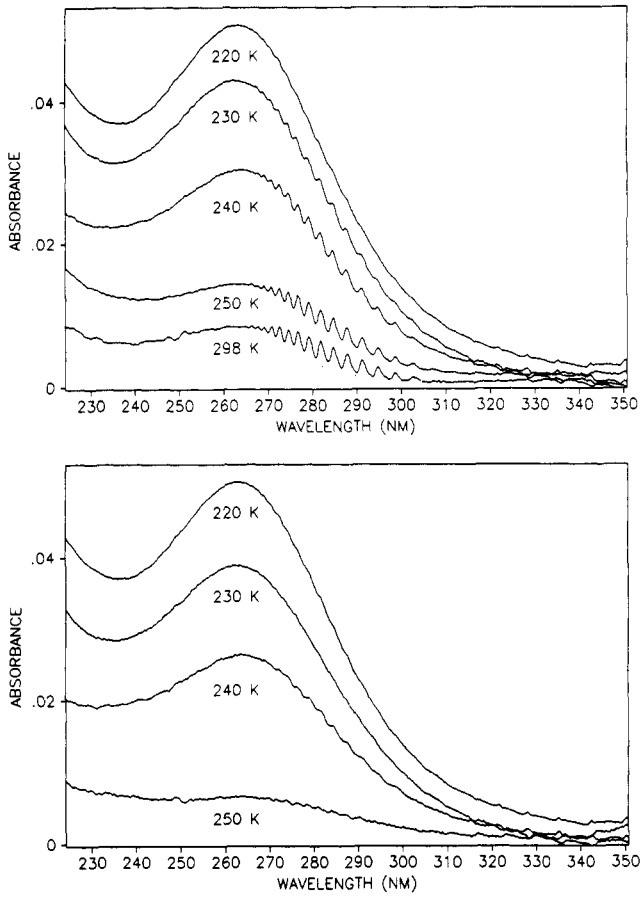

Figure 1. Ultraviolet spectra of the products of OClO + NO_3 taken between 220 and 298 K. (top) Spectra with OClO absorbance removed. (bottom) Spectra with both ClO and OClO absorbances removed. The spectrum obtained at 298 K is nearly entirely due to ClO. The remaining spectral features are presumably due to O_2ClONO_2, although variations in the spectra below 230 nm may indicate the presence of an additional absorber.

is approximately 1×10^{-13} cm^3 s^{-1}. Results of a kinetics simulation, based on one possible reaction mechanism, are presented later in this report.

UV spectra of the reaction products are shown in Figure 1. At temperatures near 298 K we observed the appearance of ClO. The production of ClO suggests the following catalytic mechanism:

$$OClO + NO_3 \rightarrow ClO + NO_2 + O_2 \quad (1a)$$

$$ClO + NO_3 \rightarrow OClO + NO_2 \quad (2a)$$

$$\text{net:} \quad 2NO_3 \rightarrow 2NO_2 + O_2$$

The rate coefficient for reaction 2a is reportedly between 1×10^{-13} and 4×10^{-13} cm^3 s^{-1}.[9,10] A second channel for reaction 2 has also been proposed,[10] namely

$$ClO + NO_3 \rightarrow ClOO + NO_2 \quad (2b)$$

The observed loss of OClO in the present experiment can be rationalized in terms of the competition between reactions 2a and 2b. The rate of ClOO in our system is dominated by rapid thermal decomposition to yield atomic chlorine and molecular oxygen followed by reaction of the atomic chlorine with either NO_3 or OClO.

$$ClOO \rightarrow Cl + O_2 \quad (3)$$

$$Cl + NO_3 \rightarrow ClO + NO_2 \quad (4)$$

$$Cl + OClO \rightarrow 2ClO \quad (5)$$

Room temperature infrared spectra of the reaction products were taken at 1-cm^{-1} resolution between 600 and 4000 cm^{-1}. The choice of instrumental resolution was dictated by signal-to-noise considerations, reactant quantity limitations, and the expectation

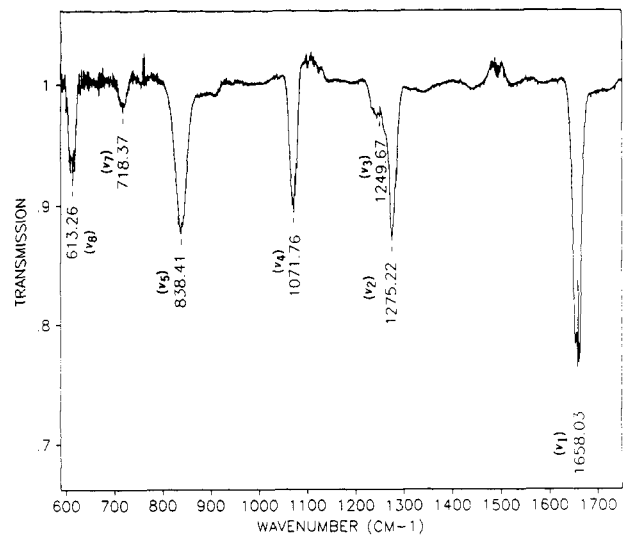

Figure 2. Infrared difference spectrum of OClO + NO_3 and NO_3 (before addition of OClO) taken at 1-cm^{-1} resolution and 220 K. The observed bands are attributed to O_2ClONO_2. Bands due to OClO have been removed. The loss of NO_3 is indicated by the positive-going bands at 762 and 1492 cm^{-1}.

that an OClO–NO_3 adduct would have no discernible rovibronic structure. All of the observed bands were attributable to NO_2, presumably a primary product associated with ClO production, and N_2O_5, a secondary product resulting from reaction of NO_2 with NO_3:

$$NO_2 + NO_3 + M \rightarrow N_2O_5 + M \quad (6)$$

Infrared transitions were not observed for ClO due to the combined effects of small ClO absorption line strengths and reduced instrumental resolution. We conclude that the observed room temperature infrared spectrum is consistent with the reaction scheme 1a, 2a, 2b, and 3–6.

As the reaction temperature was decreased below 298 K, the ultraviolet spectral features due to ClO diminished and a new ultraviolet spectrum was observed with a maximum absorption at 262 nm. The new spectrum is similar to ones observed for the higher chlorine oxides, i.e., Cl_2O_2, Cl_2O_3, and Cl_2O_4. The corresponding infrared spectrum, shown in Figure 2, consisted of seven new bands at 613.3, 718.4, 838.4, 1071.8, 1249.7, 1275.2, and 1658.0 cm^{-1}, none of which could be attributed to any of the known higher chlorine oxides.[4,11-15] The relative intensities of the seven bands remained constant for various experimental conditions, indicating the presence of only one absorbing species. We deduced that the absorbing species contains a NO_2 group from the presence of the bands at 1658.0 and 1249.7 cm^{-1} and a ClO_2 group from the presence of the bands at 1275.2 and 1071.8 cm^{-1}. On the basis of these deductions and our knowledge of the reaction system, we conclude that the unknown product is chloryl nitrate:

$$OClO + NO_3 + M \rightarrow O_2ClONO_2 + M \quad (1b)$$

Our proposed assignment of the infrared spectrum, assuming C_1 symmetry, is as follows: NO_2 a-stretch (ν_1) = 1658 cm^{-1}, NO_2 s-stretch (ν_3) = 1250 cm^{-1}, ClO_2 a-stretch (ν_2) = 1275 cm^{-1}, ClO_2 s-stretch (ν_4) = 1072 cm^{-1}; ClO stretch (ν_5) = 838 cm^{-1}; NO_2 wag (ν_7) = 718 cm^{-1}; NO stretch (ν_8) = 613 cm^{-1}.

We devised several additional experiments to test our assignment of O_2ClONO_2. First, we attempted to verify that reaction 1 was responsible for the production of the observed product. To this end we combined, at 220 K, NO_3 with Cl and ClO and OClO with NO_2. None of the new infrared bands ascribed to O_2ClONO_2 were observed in these trials. No reaction or products were observed for the OClO + NO_2 reaction. The NO_3 + Cl and NO_3 + ClO reactions produced $ClONO_2$ (from ClO + NO_2 + M) and trace amounts of OClO. The relative lack of OClO product in these experiments indicates that at 220 K the branching ratio of reaction 2 favors ClOO formation, in general agreement with the conclusion of Biggs et al.[10]

TABLE I: Experimental and Modeled Kinetics Results for OClO + NO_3[a]

			column abundance (10^{15} molecules cm^{-2})					$ClNO_5$ abs at
T (K)	P (Torr)	rxn time (s)	NO_3 initial[b]	NO_3 final[c]	OClO initial	OClO final	ClO	262 nm
298	3.9	3.2	6.5	1.0	4.7	3.3	1.2	<0.005
				(0.8)		(2.6)	(1.5)	(0.04)
	3.9	3.2	12.0	1.5	4.7	2.4	1.6	<0.005
				(1.3)		(2.0)	(1.7)	(0.05)
	3.9	3.2	15.0	2.0	4.7	2.0	2.1	<0.005
				(1.6)		(1.8)	(1.8)	(0.06)
	4.3	3.1	12.0	nm[d]	10.6	6.1	1.7	<0.005
				(1.2)		(6.4)	(2.6)	(0.09)
	4.4	2.9	10.0	1.6	17.3	13.4	1.9	<0.005
				(1.0)		(12.4)	(2.9)	(0.12)
220	3.5	4.2	8.7	0.9	5.8	3.1	<0.2	0.032
				(1.3)		(2.2)	(0.3)	(1.67)
	3.5	4.2	13.9	1.3	5.8	1.7	<0.2	0.036
				(1.8)		(1.6)	(0.4)	(2.04)
	3.7	3.9	3.5	nm	15.5	14.0	<0.2	0.010
				(0.5)		(12.6)	(0.03)	(2.11)
	3.7	3.9	12.6	nm	16.0	9.3	<0.2	0.032
				(0.8)		(7.9)	(0.2)	(3.83)
	4.3	3.5	12.6	nm	19.3	14.0	<0.2	0.061
				(1.4)		(11.4)	(0.2)	(4.61)

[a] Numbers in parentheses are column abundances (in units of 10^{15} molecules cm^{-2}) derived from the kinetics simulations using rate coefficients discussed in the text. [b] Denotes column abundance with only one reactant in cell. [c] Denotes column abundance with both reactants in cell. [d] Not measured.

As a second test, we investigated the possibility that Cl_2O_2 or Cl_2O_3 formation might account for the observed ultraviolet absorption in the NO_3–OClO reaction system:

$$ClO + ClO + M \rightarrow Cl_2O_2 + M \quad (7)$$

$$ClO + OClO + M \rightarrow Cl_2O_3 + M \quad (8)$$

We added either ClO or ClO + OClO to the reactor at 220 K and recorded ultraviolet and infrared spectra that are similar to those reported by Burkholder et al.[13] The results of these tests demonstrated that Cl_2O_2 and Cl_2O_3 could not have been solely responsible for the ultraviolet absorptions observed in the NO_3 + OClO system without producing clearly observable infrared bands.

A computer-based kinetics simulation that employed reactions 1–8 was performed on the NO_3 + OClO reaction system. The purpose of this endeavor was to further establish the plausibility of the deduced reaction mechanism and to derive refined estimates of the reaction rate parameters for reaction 1. The rate constants for reactions 1a and 1b and the branching ratio of reaction 2 were the only variable parameters in this simulation.[9,10,16] A qualitatively good description of the observed NO_3, OClO, and ClO behavior at 298 K was obtained with $k_{1a} = 2 \times 10^{-14}$ cm^3 s^{-1}, $k_{2a} = 1 \times 10^{-13}$ cm^3 s^{-1}, and $k_{2b} = 4 \times 10^{-13}$ cm^3 s^{-1}. The observed behavior of ClO as a function of temperature was best described by employing a ratio of k_{1b}/k_{1a} that increased with decreasing temperature and reached approximately 10 at 220 K. A satisfactory fit to the observed data at 220 K and 4 Torr was obtained with $k_{1a} = 2 \times 10^{-15}$ cm^3 s^{-1} and $k_{1b} = 2 \times 10^{-14}$ cm^3 s^{-1}. A summary of the experimental and modeled kinetics data is shown in Table I. In addition, we estimate that the absorption cross section for O_2ClONO_2 at 262 nm and 220 K is approximately 1.3×10^{-17} cm^2, based on the measured absorbances and the predicted column abundances shown in Table I.

The derived kinetics parameters are consistent with a recent report by Becker et al.[9] that places an upper limit of 7×10^{-14} cm^3 s^{-1} on k_1 at 298 K. However, we note that the conditions employed by Becker et al. (OClO decays in excess NO_3) should be complicated by regeneration of OClO due to reaction 2a. We are in substantial disagreement with the upper limit value of 1×10^{-15} cm^3 s^{-1} reported for k_1 by Biggs et al.[10] No experimental details are given by Biggs et al.; consequently, we are unable to critically compare the two experiments.

The derived value of k_{1b} at 220 K was used in conjunction with unimolecular reaction theory[17,18] to estimate the strength of the bond between NO_3 and OClO in O_2ClONO_2. Following the method used in ref 18, we input the following parameters for the calculation: the seven measured O_2ClONO_2 vibrational frequencies and eight additional frequencies (740, 530, 480, 355, 280, 190, 115, 100 cm^{-1}) derived from a normal-coordinate analysis[19] of O_2ClONO_2; an estimated entropy value for O_2ClONO_2 of 84 eu; an estimated energy difference of 265 cm^{-1} between the reaction enthalpy and the critical energy for O_2ClONO_2 decomposition. The O_2ClONO_2 bond strength derived from this method is 18 ± 3 kcal mol^{-1}. This value is similar to that of ClOOCl but substantially less than that of $ClONO_2$. Consequently, we expect the thermal stability of O_2ClONO_2 to approach that of ClOOCl.

Atmospheric Implications

The value derived for k_{1b} from the kinetics simulations corresponds to a third-order rate constant on the order of 10^{-31} cm^6 s^{-2}. This value is consistent with rate parameters for other known reactions of ClO_x with NO_x such as ClO + NO_2 and Cl + NO_2.[16] Accordingly, we believe that the high-pressure limit values of k_{1b} will approach 10^{-11} cm^3 s^{-1}. At temperatures and pressures characteristic of the earth's stratosphere, we expect the value of k_{1b} to be on the order of 10^{-12} cm^3 s^{-1}. In the polar stratosphere this process may serve as a significant sink for active chlorine by converting photolytically labile OClO into potentially inactive O_2ClONO_2. We have modeled the effect of reaction 1b on polar chlorine chemistry using the California Institute of Technology–Jet Propulsion Laboratory one-dimensional photochemical model[20,21] with the exception that the model atmosphere adopted is that of the "collar" region of the polar vortex,[22] where O_2ClONO_2 is expected to be most abundant. The atmospheric conditions and rate parameters used in the model were similar to those used previously.[5] The rate coefficient for the formation of O_2ClONO_2 was set equal to that of $ClONO_2$. The O_2ClONO_2 thermal decomposition rate coefficient was calculated using the formation rate coefficient and an estimate of the equilibrium constant for reaction 1b [$K_{1b} = (1 \times 10^{-28} \exp(9300/T)$] that was derived from the unimolecular theory calculation discussed previously. The photodissociation coefficient for O_2ClONO_2 was set equal to that of HNO_3 since the observed ultraviolet spectrum of O_2ClONO_2 was unmeasurably small above 300 nm.

An example of the model results[23] for noontime vertical profiles of O_2ClONO_2 is shown in Figure 3. There is little variation in the O_2ClONO_2 profile over a diurnal cycle. The concentrations of the major chlorine species ClO and $ClONO_2$ in the model are consistent with the column density constraints deduced by Toon et al.[22] in the Antarctic vortex of 1987. A sensitivity study has

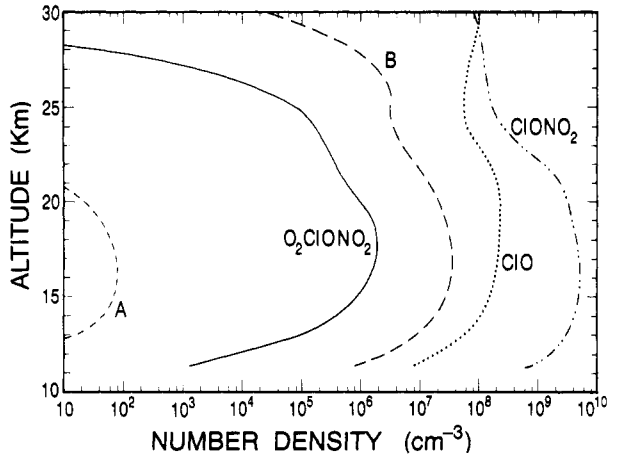

Figure 3. Model calculations of the vertical profiles of O_2ClONO_2, ClO, and $ClONO_2$ in the antarctic stratosphere during noontime conditions (second week of spring). Vertical profiles of O_2ClONO_2 labeled A and B reflect variations of ±2 kcal mol^{-1} in the estimated bond energy (see text).

been carried out on the bond energy of O_2ClONO_2. Curve A (Figure 3) shows the results for O_2ClONO_2 if the bond energy is 2 kcal mol^{-1} smaller than the standard value. Curve B gives the corresponding results if the bond energy is 2 kcal mol^{-1} larger. This large range of uncertainty is the principal source of uncertainty in the modeling of O_2ClONO_2.

The derived column densities of O_2ClONO_2 are significantly less than those obtained for $ClONO_2$ and ClO. Consideration of other reactions which form O_2ClONO_2 may increase the atmospheric abundance, however. For example, we propose that the reaction of ClO_3 with NO_2 will produce O_2ClONO_2:

$$ClO_3 + NO_2 + M \rightarrow O_2ClONO_2 + M \quad (9)$$

Currently we are investigating atmospheric pathways for formation of ClO_3.

Acknowledgment. Part of the research described in this report was carried out at the Jet Propulsion Laboratory, California Institute of Technology, under contract to the National Aeronautics and Space Administration. Y.L.Y. was supported by NASA Grant NAGW-413 to the California Institute of Technology.

References and Notes

(1) de Zafra, R. L.; Jaramillo, M.; Parrish, A.; Solomon, P.; Conner, B.; Barrett, J. *Nature* **1987**, *328*, 408.
(2) Brune, W. H.; Anderson, J. G.; Chan, K. R. *J. Geophys. Res.* **1989**, *94*, 16649.
(3) Solomon, S.; Mount, G. H.; Sanders, R. W.; Schmeltekopf, A. L. *J. Geophys. Res.* **1987**, *92*, 8329.
(4) Molina, L. T.; Molina, M. J. *J. Phys. Chem.* **1987**, *91*, 433.
(5) Sander, S. P.; Friedl, R. R.; Yung, Y. L. *Science* **1989**, *249*, 1095.
(6) Christe, K. O.; Wilson, W. W.; Wilson, R. P. *Inorg. Chem.* **1989**, *28*, 675.
(7) Friedl, R. R.; Sander, S. P. *J. Phys. Chem.* **1987**, *91*, 2721.
(8) Lang, V. I.; Sander, S. P.; Friedl, R. R. *J. Mol. Spectrosc.* **1988**, *132*, 89.
(9) Becker, E.; Wille, U.; Rahman, M. M.; Schindler, R. N. *Ber. Bunsen-Ges. Phys. Chem.* **1991**, *95*, 1173.
(10) Biggs, P.; Harwood, M. H.; Paar, A. D.; Wayne, R. P. *J. Phys. Chem.* **1991**, *95*, 7746.
(11) Schack, C. J.; Pilipovich, D. *Inorg. Chem.* **1970**, *9*, 1387.
(12) Christe, K. O.; Schack, C. J.; Curtis, E. C. *Inorg. Chem.* **1971**, *10*, 1589.
(13) Burkholder, J. B.; Orlando, J. J.; Howard, C. J. *J. Phys. Chem.* **1990**, *94*, 687.
(14) Jansen, M.; Tobias, K. M.; Willner, H. *Naturwissenschaften* **1986**, *73*, 734.
(15) Witt, J. D.; Hammaker, R. M. *J. Chem. Phys.* **1973**, *58*, 303.
(16) DeMore, W. B.; Sander, S. P.; Golden, D. M.; Molina, M. J.; Hampson, R. F.; Kurylo, M. J.; Howard, C. J.; Ravishankara, A. R. *JPL Publication 90-1*; Jet Propulsion Laboratory: Pasadena, CA, 1990.
(17) Troe, J. *J. Phys. Chem.* **1979**, *83*, 114.
(18) Colussi, A. J. *J. Phys. Chem.* **1990**, *94*, 8922.
(19) Computer analysis performed using program QCMP067 supplied by the Quantum Chemistry Program Exchange, Indiana University. The input geometrical parameters and force constants for O_2ClONO_2 were estimated from $ClONO_2$ (Miller, R. H.; Bernitt, D. L.; Hisatsune, I. C. *Spectrochim. Acta* **1967**, *23A*, 223) and Cl_2O_3 (author's unpublished data).
(20) Allen, M.; Yung, Y. L.; Waters, J. *J. Geophys. Res.* **1981**, *86*, 3617.
(21) Froidevaux, L.; Allen, M.; Yung, Y. L. *J. Geophys. Res.* **1985**, *90*, 12999.
(22) Toon, G. C.; Farmer, C. B.; Lowes, L. L.; Schaper, P. W.; Blavier, J. F.; Norton, R. H. *J. Geophys. Res.* **1990**, *94*, 16571.
(23) The maximum concentrations of ClO, BrO, and NO_x in the model are 1.5 ppbv, 5 pptv, and 10 pptv, respectively. The model results are for the beginning of September.

Polarized Fourier Transform Infrared Microscopy as a Tool for Structural Analysis of Adsorbates in Molecular Sieves

F. Schüth

Institut für Anorganische Chemie und Analytische Chemie der Johannes Gutenberg-Universität, Mainz, Becherweg 24, 6500 Mainz, Germany *(Received: May 26, 1992; In Final Form: July 28, 1992)*

Using FTIR microscopy with polarized IR radiation on silicalite I single crystals fully loaded with *p*-xylene, the existence of an ordered adsorbate could be proven for the first time by IR spectroscopy. By analyzing the polarized absorption bands the orientation of the *p*-xylene molecules relative to the host structure could be determined. The results agree well with structural data obtained from X-ray diffraction experiments. These first results suggest that polarized IR microscopy could develop into a powerful tool for the analysis of adsorbate structures, assisting in complete structure resolution by diffraction techniques.

Introduction

Polarized IR spectroscopy is a well-known technique for the analysis of orientated molecules since about 50 years ago.[1] It can be used either for assignment of IR bands to certain modes, if the orientation of molecules with respect to the IR beam is known (see, for instance, the work of Zelei and Dobos on para-substituted benzene derivatives[2-4]), or for structural analysis, if bands have already been assigned unanimously to certain modes, e.g., for orientation in polymers,[5] for analysis of details in the crystal structure[6]. To our best knowledge, however, this method has until now never been applied to analyze the orientation of adsorbates in molecular sieves. Usually for this purpose X-ray diffraction is used.[7] Occasionally also neutron diffraction[8] or one of these methods in combination with NMR spectroscopy have been applied.[9] Since experiments and data analysis in these experiments can be difficult and time consuming, it would be very advantageous to use a method which allows a relatively simple determination of the orientation of molecules in a crystal. This would exclude

0022-3654/92/2096-7493$03.00/0